International Journal of Engineering Research and Development
e-ISSN: 2278-067X, **p**-ISSN : 2278-800X, www.ijerd.com
Volume 5, Issue 1 (November 2012), PP. 46-53

A Novel Bidirectional DC-DC Converter with Battery Protection

Harinath Voruganti[1], Dr. A.Srujana[2], K.L.N.Rao[3]
[1](PG Scholar Department of EEE, Sri Venkateswara Engineering college, JNTU- Hyd, AP, INDIA)
[2] (Professor Department of EEE, Sri Venkateswara engineering college, JNTU-Hyd, AP, INDIA)
[3] (Associate Professor Department of EEE, Indur Institute of engineering&Technology, JNTU-Hyd, AP, INDIA)

Abstract:- This paper presents the implementation of a bidirectional dc-dc converter to protect a battery from overcharging and undercharging. The proposed converter circuit provides low voltage stresses across the switches, higher step-up and step-down voltage gains and efficiency is also high when compared to conventional boost/buck converter. The proposed control circuit controls the charging and discharging of the battery. The operating principle and steady state analysis for the step-up and step-down modes are discussed only in continuous conduction mode. Finally, 13/39-V prototype circuit is implemented to verify the performance of proposed converter

Keywords:- Battery, Bidirectional dc–dc converter, coupled inductor.

I. INTRODUCTION

Bidirectional dc–dc converters are used to transfer the power between two dc sources in either direction. These converters are widely used in applications, such as hybrid electric vehicle energy systems, uninterrupted power supplies, fuel-cell hybrid power systems, photovoltaic hybrid power systems, and battery chargers. Many bidirectional dc–dc converters have been researched. The bidirectional dc–dc flyback converters are more attractive due to simple structure and easy control [2], [10]. However, these converters suffer from high voltage stresses on the power devices due to the leakage inductor energy of the transformer. In order to recycle the leakage inductor energy and to minimize the voltage stress on the power devices, some literatures present the energy regeneration techniques to clamp the voltage stress on the power devices and to recycle the leakage inductor energy [11], [12]. Some literatures research the isolated bidirectional dc–dc converters, which include the half bridge [5], [6] and full-bridge types [9].These converters can provide high step-up and step-down voltage gain by adjusting the turns ratio of the transformer.

For non-isolated applications, the non-isolated bidirectional dc–dc converters, which include the conventional boost/buck [1], [4], [8], multilevel [3], three-level [7], sepic/zeta [16], switched capacitor [17], and coupled inductor types [18], are presented. The multilevel type is a magnetic-less converter, but 12 switches are used in this converter. If higher step-up and step-down voltage gains are required, more switches are needed.

The total system is useful to avoid the damage to the life of the Batteries. Because of overcharging and undercharging batteries will produce hot spots inside the battery such that the batteries not survive for long time. The following sections will describe the operating principles and steady-state analysis for the step-up and step-down modes in continuous conduction mode only. In order to analyze the steady-state characteristics of the proposed converter, some conditions are assumed: The ON-state resistance $R_{DS(ON)}$ of the switches and the equivalent series resistances of the coupled inductor and capacitors are ignored; the capacitor is sufficiently large; and the voltages across the capacitor can be treated as constant.

II. CIRCUIT CONFIGURATION AND STEADY STATE ANALYSIS

A. STEP-UP MODE

Fig. 1 shows the conventional bidirectional dc-dc boost/buck converter. The proposed converter in step-up mode is shown in Fig. 2. The pulse-width modulation (PWM) technique is used to control the switches $S_1$and S_2 simultaneously. The switch S_3 is the synchronous rectifier.

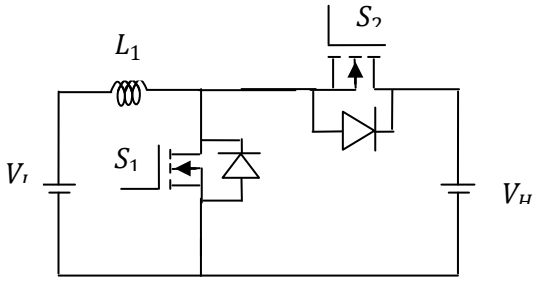

Fig1. Conventional bidirectional DC-DC boost/buck converter

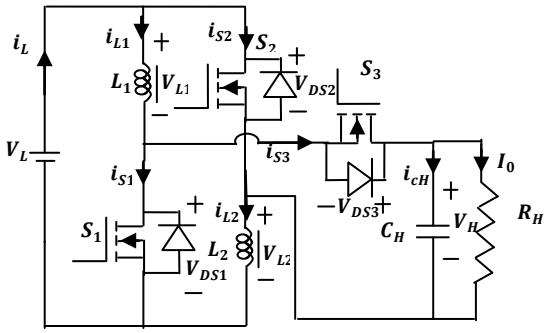

Fig.2.Proposed converter in step-up mode

Since the primary and secondary winding turns of the coupled inductor is same, the inductance of the coupled inductor in the primary and secondary sides are expressed as

$$L_1 = L_2 = L \tag{1}$$

Thus, the mutual inductance *M* of the coupled inductor is given by

$$M = k\sqrt{L_1 L_2} = kL \tag{2}$$

where k is the coupling coefficient of the coupled inductor.
The voltages across the primary and secondary windings of the coupled inductor are as follows:

$$v_{L1} = L_1 \frac{di_{L1}}{dt} + M \frac{di_{L2}}{dt} = L \frac{di_{L1}}{dt} + kL \frac{di_{L2}}{dt} \tag{3}$$

$$v_{L2} = M \frac{di_{L1}}{dt} + L_2 \frac{di_{L2}}{dt} = kL \frac{di_{L1}}{dt} + L \frac{di_{L2}}{dt} \tag{4}$$

Fig. 3 shows some typical waveforms in continuous conduction mode (CCM). The operating principles and steady-state analysis of CCM is described as follows.

1) Mode 1: During this time interval $[t_0, t_1]$, S_1 and S_2 are turned on and S_3 is turned off. The energy of the low-voltage side V_L is transferred to the coupled inductor. Meanwhile, the primary and secondary windings of the coupled inductor are in parallel. The energy stored in the capacitor C_H is discharged to the load. Thus, the voltages across L_1 and $L_2$are obtained as

$$v_{L1} = v_{L2} = V_L \tag{5}$$

Substituting (3) and (4) into (5), yielding

$$\frac{di_{L1}(t)}{dt} = \frac{di_{L2}(t)}{dt} = \frac{V_L}{(1+k)L}, \quad t_0 \le t \le t_1 \tag{6}$$

2) Mode 2: During this time interval $[t_1, t_2]$, S_1 and S_2 are turned off and S_3 is turned on. The low-voltage side V_L and the coupled inductor are in series to transfer their energies to the capacitor C_H and the load. Meanwhile, the primary and secondary windings of the coupled inductor are in series. Thus, the following equations are found to be

$$i_{L1} = i_{L2} \tag{7}$$

$$v_{L1} + v_{L2} = V_L - V_H \tag{8}$$

Substituting (3), (4), and (7) into (8), yielding

$$\frac{di_{L1}(t)}{dt} = \frac{di_{L2}(t)}{dt} = \frac{V_L - V_H}{2(1+k)L}, \quad t_1 \le t \le t_2 \tag{9}$$

By using the state-space averaging method, the following equation is derived from (6) and (9):

$$\frac{DV_L}{(1+k)L} + \frac{(1-D)(V_L - V_H)}{2(1+k)L} = 0 \tag{10}$$

Simplifying (10), the voltage gain is given as

$$G_{CCM(step-up)} = \frac{V_H}{V_L} = \frac{1+D}{1-D} \qquad (11)$$

.

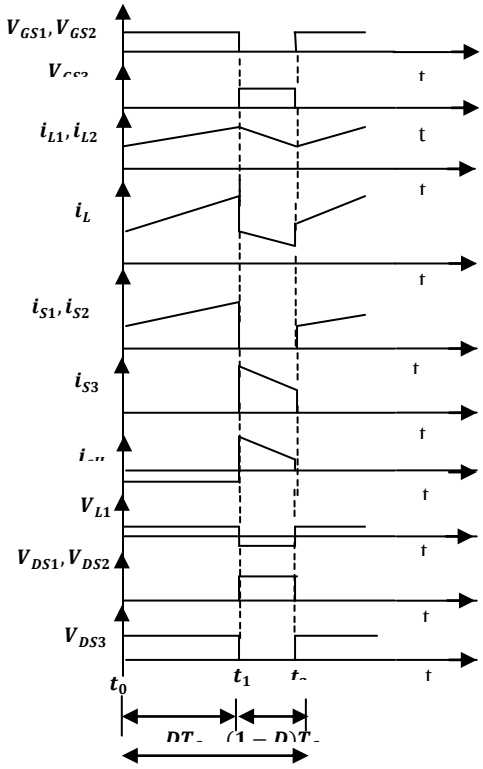

Fig.3. waveforms of proposed converter in step-up mode in CCM mode of operation

B. STEP-DOWN MODE

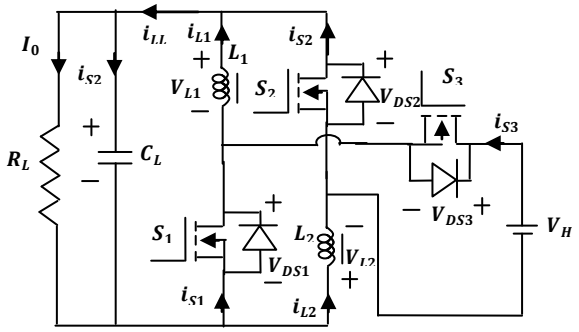

Fig.4.Proposed converter in step-down mode

Fig. 4 shows the proposed converter in step-down mode. The PWM technique is used to control the switch S_3. The switches S_1 and S_2 are the synchronous rectifiers. Fig. 5 shows some typical waveforms in CCM. The operating principle and steady-state analysis of CCM is described as follows.

1) Mode 1: During this time interval $[t_0,t_1]$ S_3 is turned on and S_1/S_2 are turned off. The energy of the high-voltage side V_H is transferred to the coupled inductor, the capacitor C_L, and the load. Meanwhile, the primary and secondary windings of the coupled inductor are in series. Thus, the following equations are given as:

$$i_{L1} = i_{L2} \qquad (12)$$

$$v_{L1} + v_{L2} = V_H - V_L \qquad (13)$$

Substituting (3), (4), and (12) into (13), yielding

$$\frac{di_{L1}(t)}{dt} = \frac{di_{L2}(t)}{dt} = \frac{V_H - V_L}{2(1+k)L}, \quad t_0 \le t \le t_1 \qquad (14)$$

2) Mode 2: During this time interval $[t_1, t_2]$, S_3 is turned off and S_1 /S_2 are turned on. The energy stored in the coupled inductor is released to the capacitor C_L and the load. Meanwhile, the primary and secondary windings of the coupled inductor are in parallel. Thus, the voltages across L_1 and L_2 are derived as

$$v_{L1} = v_{L2} = -V_L \tag{15}$$

Substituting (3) and (4) into (15), yielding

$$\frac{di_{L1}(t)}{dt} = \frac{di_{L2}(t)}{dt} = -\frac{V_L}{(1+k)L}, \quad t_1 \le t \le t_2 \tag{16}$$

By using the state space averaging method, the following equation is obtained from (14) and (16):

$$\frac{D(V_H - V_L)}{2(1+k)L} - \frac{(1-D)V_L}{(1+k)L} = 0 \tag{17}$$

Simplifying (17), the voltage gain is found to be

$$G_{CCM(step-down)} = \frac{V_L}{V_H} = \frac{D}{2-D} \tag{18}$$

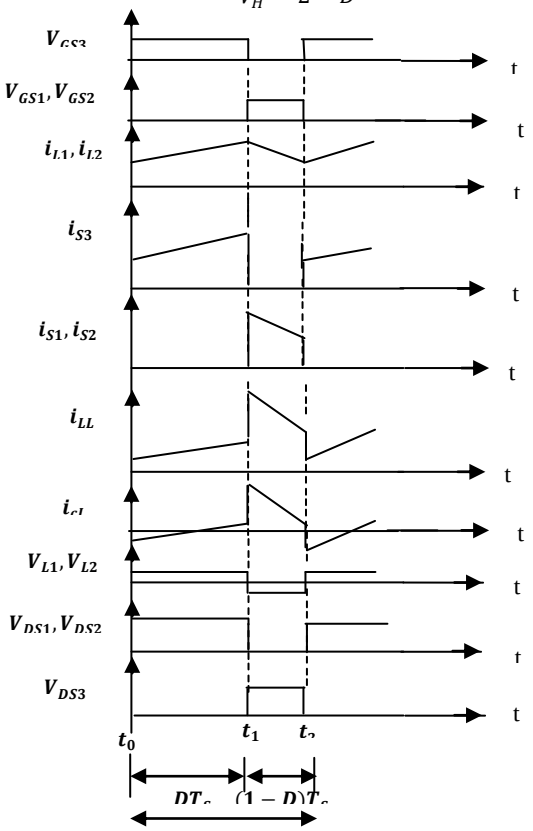

Fig.5. waveforms of proposed converter in step-down mode in CCM mode of operation

III. ANALYSIS OF BATTERY PROTECTION

The basic model of a battery is shown in the fig.6.

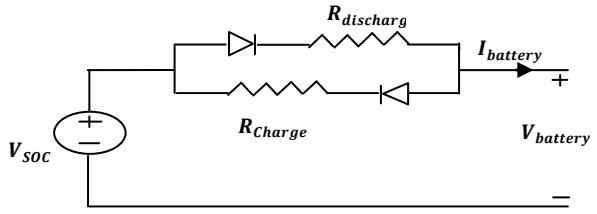

Fig.6. basic model of a battery

With the current flow in the battery there is some resistive drop in electrodes and resistance offered to the movement of ions, are modeled as electrical resistances here. Battery capacity is defined as the current that discharges in 1hour. So the battery capacity should be in Ampere-hours. In practice the relationship between battery capacity and discharge current is not linear.

Peukert's Law relates battery capacity to discharge rate:

$$C = I^k t \qquad (19)$$

where C is the battery capacity, I is the discharge current, t is the discharge time, k is the Peukert coefficient, typically 1.1to 1.3. The output voltage of the bidirectional dc-dc converter is connected to the three Lead-Acid batteries which are connected in series.

Table-1: charge limits of a 12V battery

	Fully charged	Discharged completely
State of charge	100%	0%
Voltage	12.7V	11.6V

Let a single battery fully charged voltage is V_1 and completely discharged voltage will be V_2 . Here three batteries of V_1 each are connected in series so that the fully charge voltage (3xV_1) V is the overcharged voltage. Similarly (3xV_2) V is the undercharged voltage.

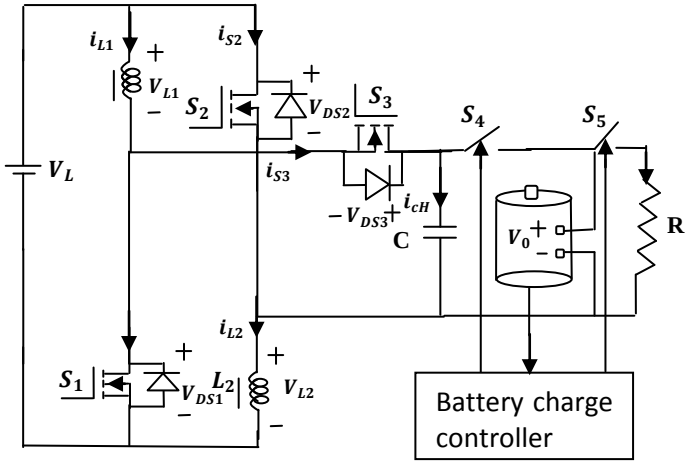

Fig.7. Battery charge controller in step-up mode

Initially S_4 and S_5 both switches are in closed condition. Whenever the voltage across batteries is greater than or equal to (3xV_1) V, switch S_4 will open. Under this condition load will fed from the batteries. Means under overcharged condition supply to batteries and load from the bidirectional dc-dc converter is disconnected. While discharging if the voltage across the batteries is less than or equal to (3xV_2) V switch S_5 will open.

The total system is useful to avoid the damage to the life of batteries. Because of overcharging and undercharging batteries will not survive for long time.

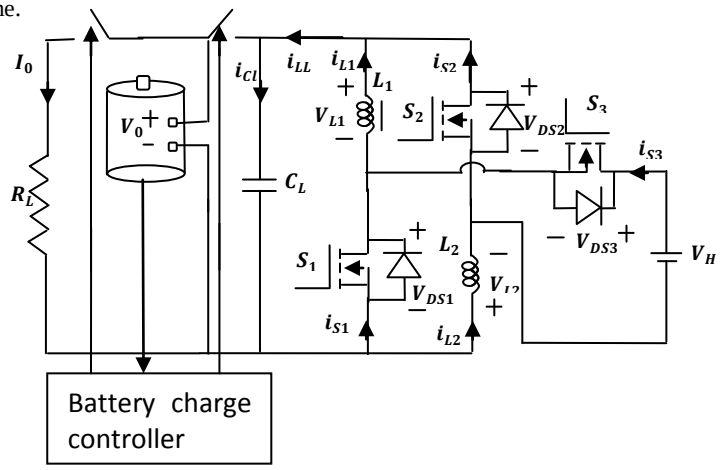

Fig.8. Battery charge controller in step-down mode

The output voltage of the bidirectional dc-dc converter is connected to a single Lead-Acid battery.
The output voltage across the battery is limited by the battery charge controller so that controlling the charging and discharging of the battery. The operation principle is same as in step-up mode.

IV. EXPERIMENTAL RESULTS

Simulation of novel bidirectional dc-dc converter with battery protection was performed by using MATLAB SIMULNK to confirm the above analysis. The electric specifications and circuit components are selected as V_L = 13 V, V_H = 39 V, f_S = 50 kHz, P_0= 200 W, C_L = C_H = 330 μF, L_1 = L_2 =15.5 μH (r_{L1} = r_{L2}= 11 mΩ). Also, MOSFET IRF3710 (V_{DSS} = 100 V, $R_{DS(ON)}$) = 23 mΩ, and I_D = 57 A) is selected forS_1,S_2 and S_3.

Some experimental results in step-up mode are shown in Figs. 9-15. Fig.9 shows the waveform of the output voltage across the battery. It shows that the voltage across the battery is limited in the range of overcharging and undercharging levels. Fig.10 shows the waveform of the input current. Figs.11 and 12 and 13 show the switch currents across the switches. Fig. 14 shows the waveform of the coupled-inductor i_{L1} and fig.15 shows the coupled-inductor current i_{L2}. The source current is double of the level of the coupled-inductor current during S_1 /S_2 ON-period and equals the coupled-inductor current during S_1 /S_2 OFF-period. It can be observed that i_{L1} is equal to i_{L2}. The source current equals to the coupled-inductor current during S_3 ON-period and is double of the level of the coupled-inductor current during S_3 OFF-period. Fig.16 shows the output voltage across the battery.

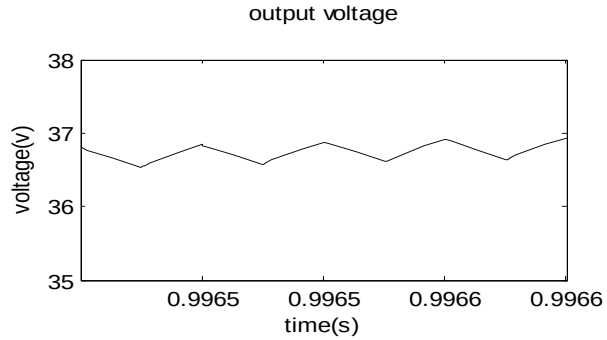

Fig.9. simulation result for the output voltage

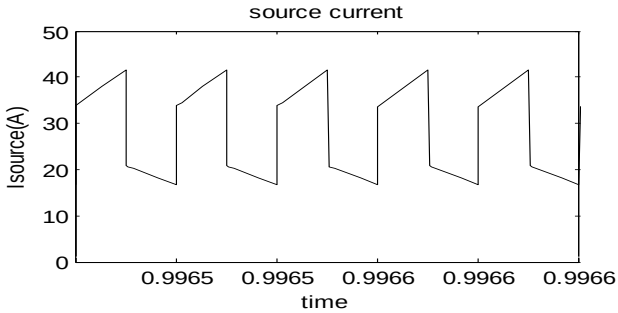

Fig.10. simulation waveform for the source current

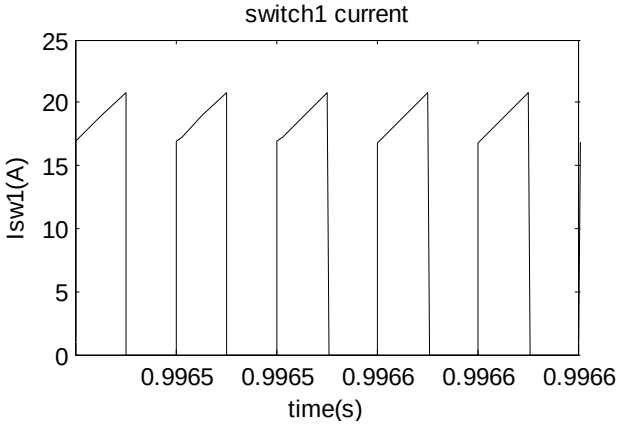

Fig.11. simulation result for the switch1 current

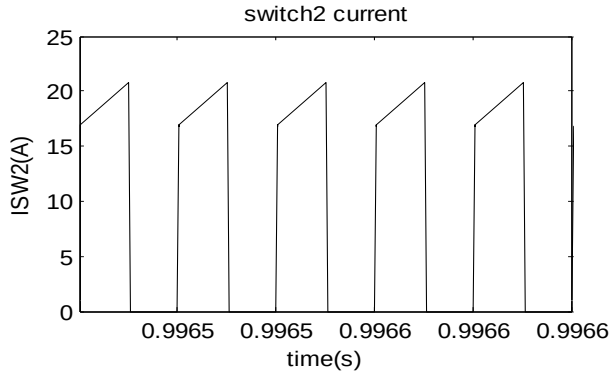

Fig.12. simulation result for the switch2 current

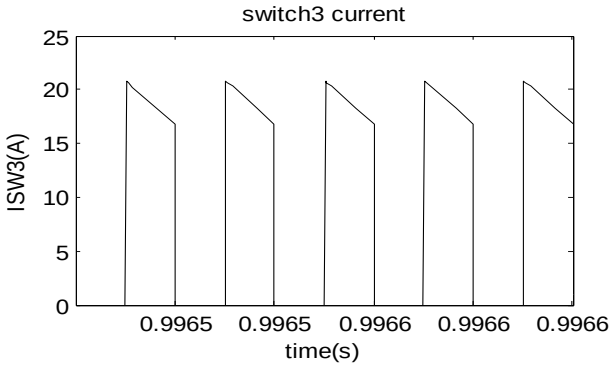

Fig.13. simulation result for the switch3 current

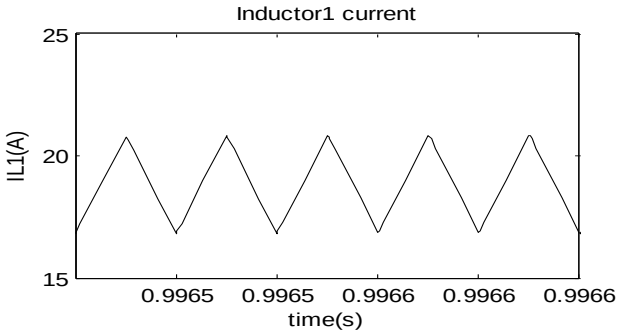

Fig.14. simulation result for the coupled inductor1 current

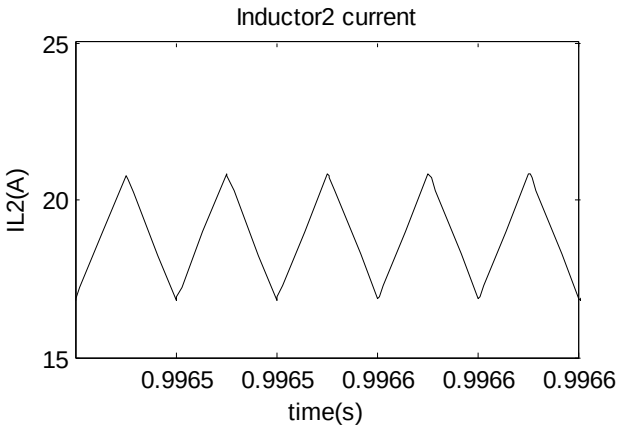

Fig.15. simulation result for the coupled inductor2 current

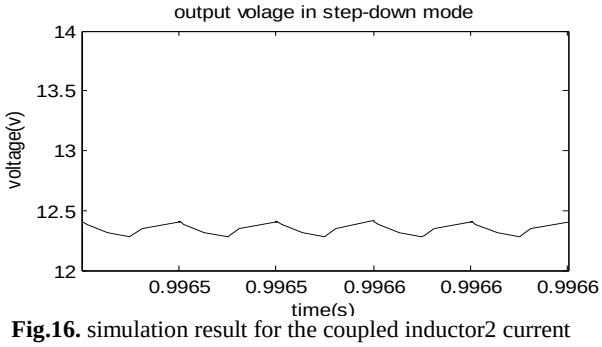

Fig.16. simulation result for the coupled inductor2 current

V. CONCLUSION

In this paper, a novel bidirectional dc–dc converter with battery protection is proposed. The circuit configuration of the proposed converter is very simple. The operation principle, including the operation modes and steady-state analysis is explained in detail. The proposed converter has higher step-up and step-down voltage gains and lower average value of the switch current than the conventional bidirectional boost/buck converter. From the experimental results, it is see that the experimental waveforms agree with the operating principle and steady-state analysis.

REFERENCES

[1]. M. B. Camara, H. Gualous, F. Gustin, A. Berthon, and B. Dakyo, "DC/DC converter design for supercapacitor and battery power management in hybrid vehicle applications—Polynomial control strategy," *IEEE TransInd. Electron.*, vol. 57, no. 2, pp. 587–597, Feb. 2010.

[2]. T. Bhattacharya, V. S. Giri, K. Mathew, and L. Umanand, "Multiphase bidirectional flyback converter topology for hybrid electric vehicles," *IEEE Trans. Ind. Electron.*, vol. 56, no. 1, pp. 78–84, Jan. 2009.

[3]. F. Z. Peng, F. Zhang, and Z. Qian, "A magnetic-less dc–dc converter for dual-voltage automotive systems," *IEEE Trans. Ind. Appl.*, vol. 39, no. 2, pp. 511–518, Mar./Apr. 2003.

[4]. [4] A. Nasiri, Z. Nie, S. B. Bekiarov, and A. Emadi, "An on-line UPS system with power factor correction and electric isolation using BIFRED converter," *IEEE Trans. Ind. Electron.*, vol. 55, no. 2, pp. 722–730, Feb. 2008.

[5]. G. Ma, W. Qu, G. Yu, Y. Liu, N. Liang, and W. Li, "A zero-voltageswitching bidirectional dc–dc converter with state analysis and softswitching-oriented design consideration," *IEEE Trans. Ind. Electron.*,vol. 56, no. 6, pp. 2174–2184, Jun. 2009.

[6]. F. Z. Peng, H. Li, G. J. Su, and J. S. Lawler, "A new ZVS bidirectional dc–dc converter for fuel cell and battery application," *IEEE Trans. Power Electron.*, vol. 19, no. 1, pp. 54–65, Jan. 2004.

[7]. K. Jin, M. Yang, X. Ruan, and M. Xu, "Three-level bidirectional converter for fuel-cell/battery hybrid power system," *IEEE Trans. Ind. Electron.*, vol. 57, no. 6, pp. 1976–1986, Jun. 2010.

[8]. Z. Liao and X. Ruan, "A novel power management control strategy for stand-alone photovoltaic power system," in *Proc. IEEE IPEMC*, 2009, pp. 445–449.

[9]. S. Inoue and H. Akagi, "A bidirectional dc–dc converter for an energy storage system with galvanic isolation," *IEEE Trans. Power Electron.*, vol. 22, no. 6, pp. 2299–2306, Nov. 2007.

[10]. K. Venkatesan, "Current mode controlled bidirectional flyback converter," in *Proc. IEEE Power Electron. Spec. Conf.*, 1989, pp. 835–842. [11] G. Chen, Y. S. Lee, S. Y. R. Hui, D. Xu, and Y. Wang, "Actively clamped bidirectional flyback converter," *IEEE Trans. Ind. Electron.*, vol. 47, no. 4, pp. 770–779, Aug. 2000.

[11]. F. Zhang and Y. Yan, "Novel forward-flyback hybrid bidirectional dc–dc converter," *IEEE Trans. Ind. Electron.*, vol. 56, no. 5, pp. 1.

[12]. H. Li, F. Z. Peng, and J. S. Lawler, "A natural ZVS medium-power bidirectional dc–dc converter with minimum number of devices," *IEEE Trans. Ind. Appl.*, vol. 39, no. 2, pp. 525–535, Mar. 2003.

[13]. B. R. Lin, C. L. Huang, and Y. E. Lee, "Asymmetrical pulse-width modulation bidirectional dc–dc converter," *IET Power Electron.*, vol. 1, no. 3, pp. 336–347, Sep. 2008.

[14]. Y. Xie, J. Sun, and J. S. Freudenberg, "Power flow characterization of a bidirectional galvanically isolated high-power dc/dc converter over a wide operating range," *IEEE Trans. Power Electron.*, vol. 25, no. 1, pp. 54–66, Jan. 2010.

[15]. I. D. Kim, S. H. Paeng, J. W. Ahn, E. C. Nho, and J. S. Ko, "New bidirectional ZVS PWM sepic/zeta dc–dc converter," in *Proc. IEEE ISIE*, 2007, pp. 555–560.

[16]. Y. S. Lee and Y. Y. Chiu, "Zero-current-switching switched-capacitor bidirectional dc–dc converter," *Proc. Inst. Elect. Eng.—Elect. Power Appl.*, vol. 152, no. 6, pp. 1525–1530, Nov. 2005.

[17]. R. J. Wai and R. Y. Duan, "High-efficiency bidirectional converter for power sources with great voltage diversity," *IEEE Trans. Power Electron.*, vol. 22, no. 5, pp. 1986–1996, Sep. 2007.

[18]. L. S. Yang, T. J. Liang, and J. F. Chen, "Transformerless dc–dc converters with high step-up voltage gain," *IEEE Trans. Ind. Electron.*, vol. 56, no. 8, pp. 3144–3152, Aug. 2009.578–1584, May 2009.